Talanta 84 (2011) 607–613

Contents lists available at ScienceDirect

Talanta

journal homepage: www.elsevier.com/locate/talanta

Fe_2O_3@Au core/shell nanoparticle-based electrochemical DNA biosensor for *Escherichia coli* detection

Kang Li, Yanjun Lai, Wen Zhang, Litong Jin*

Department of Chemistry, East China Normal University, Shanghai 200062, PR China

ARTICLE INFO

Article history:
Received 18 October 2010
Received in revised form
15 December 2010
Accepted 21 December 2010
Available online 8 January 2011

Keywords:
Fe_2O_3@Au core/shell nanoparticles
Escherichia coli (*E. coli*)
Electrochemical DNA biosensor
Horseradish peroxidase (HRP)

ABSTRACT

A Fe_2O_3@Au core/shell nanoparticle-based electrochemical DNA biosensor was developed for the amperometric detection of *Escherichia coli* (*E. coli*). Magnetic Fe_2O_3@Au nanoparticles were prepared by reducing $HAuCl_4$ on the surfaces of Fe_2O_3 nanoparticles. This DNA biosensor is based on a sandwich detection strategy, which involves capture probe immobilized on magnetic nanoparticles (MNPs), target and reporter probe labeled with horseradish peroxidase (HRP). Once magnetic field was added, these sandwich complexes were magnetically separated and HRP confined at the surfaces of MNPs could catalyze the enzyme substrate and generate electrochemical signals. The biosensor could detect the concentrations upper than 0.01 pM DNA target and upper than 500 cfu/mL of *E. coli* without any nucleic acid amplification steps. The detection limit could be lowered to 5 cfu/mL of *E. coli* after 4.0 h of incubation.

1. Introduction

Escherichia coli (*E. coli*) is the most common intestinal microorganism of humans and other warm-blooded animals and its presence is routinely used as an indicator to monitor potential enteric pathogen contamination of waters. *E. coli* may cause illness ranging from mild watery diarrhea to life-threatening conditions, such as hemolytic uremic syndrome, hemorrhagic colitis and even septicemia [1]. Conventional microbiological detection of *E. coli* includes plate counting, multiple-tube fermentation, membrane filter technique and turbidimetry [2–4]. These methods are still the most definite, but the drawbacks of long incubation time (1–2 days) and complex operation are unignorable. Therefore, the development of rapid, sensitive, simple and inexpensive detection methods of *E. coli* is very important in the fields of environmental monitoring, food industry and clinic chemistry.

Researchers have developed a number of new methods based on various measuring principles, such as polymerase chain reaction [5,6], immunoassay [7,8], chemiluminescence assay and fluorescence method [9,10], etc. In the last few years, a variety of sensitive DNA or RNA biosensors have been widely applied in the detection of bacteria, viruses and various chemical substances [11–13], with attractive features of excellent selectivity, high sensitivity, portability and low cost [14,15]. Reports about the utilization of electrochemical DNA biosensor for the detection and enumeration of *E. coli* are already being investigated [16–18].

Magnetic nanoparticles (MNPs) owe their popularity to their strong magnetic properties, high separation efficiency, and high specific surface area, offering a versatile tool for electrochemical DNA and protein biosensing. They can be easily separated from liquid phase with a magnet and again dispersed immediately with the magnet removed, which makes possible the process of modification and hybridization to be conducted away from the electrode surface, avoiding nonspecific adsorptions at the sensor [19]. Among them, iron oxide nanoparticles have been extensively studied. However their applicability is notably hindered by their spontaneous oxidizable surface and biomolecules immobilization often involves complicated synthetic procedures to chemically modify the material's surfaces [20]. To overcome these limitations, Au-coated Fe oxide nanoparticles have been fabricated to open wider possibilities of surface functionality and at the same time reduce surface oxidation [21,22]. Considerable attention has been paid to Au nanoparticles due to their high stability, biocompatibility and the capacity to combine with other molecules [23]. Especially Au-thiol chemistry can be utilized as a platform for introducing thiolated biomolecules, all the while maintaining the magnetic utility of the core; thus, widening their applicability in biotechnology significantly [24]. The further application of the Fe oxide@Au MNPs would be exploited in this study.

In this contribution, we proposed an efficient, sensitive amperometric DNA biosensor based on Fe_2O_3@Au MNPs for *E. coli* detection. Fe_2O_3@Au MNPs were used as the DNA supporters and the magnetic separation mediums. A sandwich-type assay was designed for DNA detection, which involved a pair of DNA probes (capture and reporter probes) that flanked the target probe. Such dual hybridization processes significantly improved the signal-to-

* Corresponding author. Tel.: +86 21 62232627; fax: +86 21 62232627.
E-mail address: ltjin@chem.ecnu.edu.cn (L. Jin).

0039-9140/$ – see front matter
doi:10.1016/j.talanta.2010.12.042

Table 1
Sequences of oligonucleotides employed in this work.

Name	Sequences
Capture probe	5′-SH-TAT TAA CTT TAC TCC-3′
Reporter probe	5′-CTT CCT CCC CGC TGA -BIOTIN-3′
Target probe	5′-TCA GCG GGG AGG AAG GGA GTA AAG TTA ATA-3′
Single base mis-matched probe	5′-TCA GCG GGG AGG ACG GGA GTA AAG TTA ATA-3′
Four base mis-matched probe	5′-TCA GTG GGA AGG AAT GGA GTA CAG TTA ATA-3′
Non-complementary probe	5′-GCC ATG CAA TAC CCT TCA ACA CTG TAA ACA-3′

noise ratio. The detection limit could be further pushed down by using horseradish peroxidase (HRP) as an enzyme amplify label [25] and 3,3′,5,5′-tetramethylbenzidine (TMB) which functions as a co-substrate. The new strategy thus incorporates the high sensitivity and the high selectivity attribute of nanoparticle-based electrical assays. Such electrochemical biosensor holds great promise for highly sensitive detection of DNA hybridization and measurements of *E. coli*.

2. Experimental

2.1. Chemicals

All synthetic oligonucleotides were purchased from Sangon Inc. (Shanghai, China), and their sequences are shown in Table 1. Target DNA is a segment from the 16S rRNA. Avidin-HRP and TMB were purchased from Sigma–Aldrich. Avidin-HRP was dissolved in 0.01 M phosphate buffered saline, pH 7.4, containing 0.01% thimerosal. Buffer solutions used in these experiments are as follows: DNA immobilization buffer (10 mM Tris–HCl, 1 mM EDTA and 1 M NaCl, pH 7.4); washing buffer (0.01 M NaCl and 5 mM Tris–HCl, pH 7.4); hybridization buffer (1 M NaCl and 10 mM Tris–EDTA buffer, pH 7.4); DNA stock solution (10 mM phosphate sodium buffer, pH 7.4, 100 mM NaCl, 1% BSA (bovine serum albumin), 0.01% thiomersal). *E. coli* DH5α was from School of Life Sciences, East China Normal University (Shanghai, China). Luria broth (LB) medium contains 1.0% of tryptone, 0.5% of sodium chloride and 0.5% of yeast extract. TIANamp Bacteria DNA Kit was from TIANGEN BIOTECH (Beijing, China). All other chemicals were analytical grade or better. All solutions were prepared with doubly distilled water.

2.2. Apparatus

Electrochemical measurements were performed on a CHI 660c electrochemical analyzer (CHI Instruments, Chenhua, Shanghai, China) with a three-electrode system consisting of an Ag/AgCl/3.0 M KCl as the reference electrode, a platinum wire electrode as the auxiliary electrode and a glassy carbon electrode as the working electrode. A transmission electron microscopy (TEM, JEM-2010, JEOL, Japan) was used to characterize the MNPs. The XRD patterns were collected on a Bruker D8 ADVANCE instrument using Cu Kα radiation. UV–visible spectra of the MNPs were measured at the wavelength ranging from 350 to 800 nm at room temperature.

2.3. The fabrication of Fe_2O_3@Au MNPs

As partially oxidized Fe_3O_4 nanoparticles are more resistant to Au deposition than Fe_2O_3 particles, Au^{3+} reduction may preferentially occur at more oxidized sites [22]. We choose to fabricate Fe_2O_3@Au core/shell nanoparticles by deposition of Au on the preformed Fe_2O_3 nanoparticles using a modification of Lyon's iterative hydroxylamine seeding procedure. Volumes of 0.17 mL of 12.1 M HCl and 5 mL of purified, deoxygenated water (by nitrogen gas bubbling for 10 min) were combined, and 1.04 g of $FeCl_3{\cdot}6H_2O$ and 0.4 g of $FeCl_2{\cdot}4H_2O$ were successively dissolved in the solution with stirring. The resulting solution was added dropwise into 50 mL of 1.5 M NaOH solution under vigorous stirring at 80 °C. An instant black precipitate was generated. The stirring was kept on, until the solution was cooled to room temperature. The paramagneticity was checked in situ by placing a magnet near the black precipitate of Fe_3O_4. The precipitate was isolated in the magnetic field, and the supernatant was removed by decantation. After being washed three times with water, 100 mL of 0.01 M HCl solution was added into the precipitate (with stirring) to neutralize the anionic charges on the nanoparticles. The resulting colloidal was again isolated by the magnet and washed twice by water. The fresh Fe_3O_4 nanoparticles were then dispersed in 50 mL of 0.01 M HNO_3 and heated with stirring at 90–100 °C for 1 h to completely oxidize the particles to Fe_2O_3. During heating, the color of the solution changed from brownish black to brownish red. The solution was allowed to cool to room temperature and rinsed using water followed by ethanol. The final precipitate was dispersed in 50 mL ethanol and stored at 4 °C.

0.75 mL of Fe_2O_3 colloidal was diluted in 14 mL water, and then stirred with 0.75 mL of 0.1 M sodium citrate for 10 min. 0.2 M $NH_2OH{\cdot}HCl$ and 1% $HAuCl_4$ were then added incrementally. Five additions (each for $NH_2OH{\cdot}HCl$ and $HAuCl_4$) were totally performed during the reaction, and the stirring continued for at least 50 min after each addition. The solution became blue at first addition and gradually changed to garnet during the successive iterations. The resultant Fe_2O_3@Au MNPs were separated from the solution by the magnet and washed twice by water and ethanol, respectively. The Fe_2O_3@Au MNPs were resuspended with 5 mL of ethanol and can be stored in refrigerators for at least a month.

2.4. Preparation of DNA coated MNPs

1 mL of Fe_2O_3@Au nanoparticle solution was taken for DNA immobilization. The solid phase was separated from the aqueous phase by magnetic settlement and rinsed twice with doubly distilled water. Subsequently, 50 μM thiolated DNA (capture probe dissolved in the DNA immobilization buffer) was added to the nanoparticles (final concentration of DNA was 5 μM). The mixture was stirred overnight at 25 °C. 100 μL of 10% BSA solution was added to block the surfaces of the nanoparticles and 30 min later, the unbound oligonucleotides and BSA were removed easily by using a magnet. The capture probe coated MNPs were washed with the washing buffer for three times and suspended in 500 μL stock solution at 4 °C for further use.

2.5. Bacteria cultivation and counting

E. coli DH5α cultures were grown overnight in LB medium at 37 °C with aeration by shaking, which allowed the growing stationary phase to be reached. For detecting the density of *E. coli*, the stationary phase *E. coli* cultures were serially diluted (10-fold steps) 10^7 times with LB medium and 100 μL diluted solution of *E. coli* was plated on LB agar plates. After incubation at 37 °C for 24 h, *E. coli* colonies on plates were counted to determine the number of colony-forming units per milliliter (cfu/mL). Glass apparatus, LB medium and doubly distilled water, etc. used in this section were sterilized at 120 °C for 20 min.

2.6. DNA extraction

For the detection of *E. coli* DH5α, its genomic DNA was isolated by using TIANamp Bacteria DNA Kit. *E. coli* genomic DNA solution was denatured by being heated in a water bath (80 °C) for 1 min and was immediately chilled in ice to obtain denatured single-stranded DNA. The single-stranded DNA product should be stored at −20 °C to prevent its degradation. The DNA samples were utilized for hybridization studies.

2.7. DNA hybridization and detection

In a typical experiment, 25 μL capture probe coated MNPs were added to a 1.5 mL centrifuge tube, which was previously passivated by 5% BSA for 1 h. The MNPs were washed with hybridization buffer, and magnetically collected. 85 μL of hybridization buffer containing various amounts of target DNA, 5 μL of 10% BSA and 10 μL of biotinylated reporter probe (100 nM) were mixed and incubated with the nanoparticles for 40 min at 40 °C under shaking. The nanoparticles were rinsed with the washing buffer and then incubated with 2 μL of avidin-HRP (0.5 U/mL) for 15 min at room temperature. The resulting complexes were magnetically collected and rinsed with washing buffer. This washing procedure was repeated five times to remove unbound molecules.

The substrate solution for electrochemical measurements consisted of 2×10^{-4} mol/L TMB and 10^{-3} mol/L H_2O_2 in 0.1 mol/L citrate–phosphate buffer (pH 5.0). H_2O_2 was added to the TMB solution just before the measurement. 250 μL of the TMB substrate solution was added to react with the resulting complexes for 1 min at room temperature under stirring. Amperometric detection was performed with a fixed potential of 100 mV, and the steady state was usually reached and recorded within 100 s.

3. Results and discussion

3.1. Characterization of Fe_2O_3@Au core/shell nanoparticles

The sizes and compositions of the Fe_2O_3@Au MNPs were analyzed using TEM, as shown in Fig. 1. Particle diameters were determined by measuring the long axis of each particle. The average diameter of the Fe_2O_3 nanoparticles (Fig. 1A) is 9 ± 3 nm; addition of $HAuCl_4$ and hydroxylamine increases the average diameter and affects the surface morphology. The measured average diameter of Fe_2O_3@Au nanoparticles (Fig. 1B) is 20 ± 5 nm and the Au shell of about 10 nm coated well outside of iron oxide was evidenced. It can also be concluded that the reduction of Au^{3+} may produce more spherical particles.

UV–visible absorption spectra of colloid Au, Fe_2O_3 and Fe_2O_3@Au nanoparticles are observed in Fig. 2. The synthesized colloid Au has a characteristic absorption peak at 520 nm, deducing that the diameter of Au was distributed around 3–20 nm [26]. The Fe_2O_3 nanoparticles have no characteristic absorption in the examined range. However, after the MNPs were coated with Au shell, a plasmon absorption peak at 548 nm was remarkably observed, indicating that the Fe_2O_3@Au MNPs were formed. The red-shift comparing with pure Au particles may result from the increased size of Au nanoparticles and deficient electron population on Au due to the interfacial communication between Au and Fe oxide [27–29].

The crystal structure of the samples was analyzed by X-ray diffraction (XRD). Fig. 3 displays the XRD patterns of (A) Fe_2O_3 and (B) Fe_2O_3@Au MNPs. The XRD pattern of Fe_2O_3 nanoparticles depicts diffraction peaks at 30.05°, 35.33°, 43.01°, 53.39°, 56.87° and 62.48° (almost the same as Fe_3O_4 nanoparticles), which can be indexed to the (2 2 0), (3 1 1), (4 0 0), (4 2 2), (5 1 1) and (4 4 0) planes of Fe_3O_4 in a cubic phase, respectively. The values obtained agree well with the standard peak values of XRD pattern of Fe_3O_4 (Joint Committee on Powder Diffraction Standards, JCPDS 19-0629). The data for the Fe_2O_3@Au nanoparticles exhibits diffraction peaks at 38.2°, 44.4°, 64.6° and 77.5°, which can be indexed to the (1 1 1), (2 0 0), (2 2 0) and (3 1 1) planes of gold cubic phase, respectively (JCPDS 04-0784). The Au-shell sample also demonstrates four weak peaks (2 2 0), (3 1 1), (5 1 1) and (4 4 0) of Fe_2O_3. The penetration of X-rays through the gold-coated layer to the central Fe_2O_3 core can reveal the diffraction peaks for Fe_2O_3 [30]. The absence of any diffraction peaks for magnetite is most likely due to the heavy atom effect from gold as a result of the formation of Au-coated Fe_2O_3 nanoparticles. The XRD pattern with the diffraction peaks

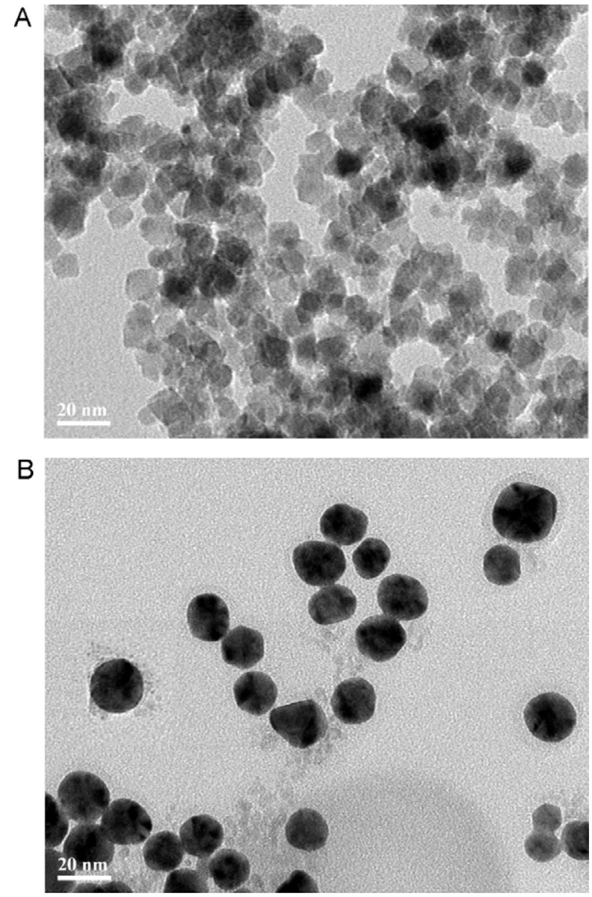

Fig. 1. TEM images of (A) Fe_2O_3 and (B) Fe_2O_3@Au MNPs.

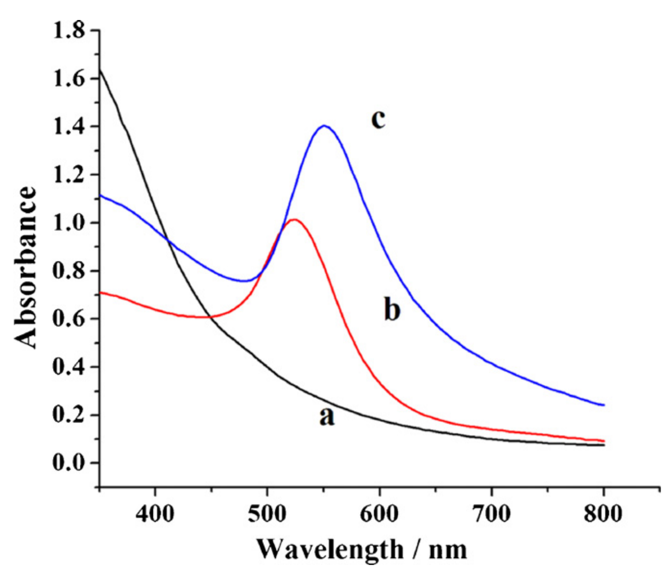

Fig. 2. The UV–visible absorption spectra of the different colloid: Fe_2O_3 (a), Au (b) and Fe_2O_3@ Au (c) nanoparticles.

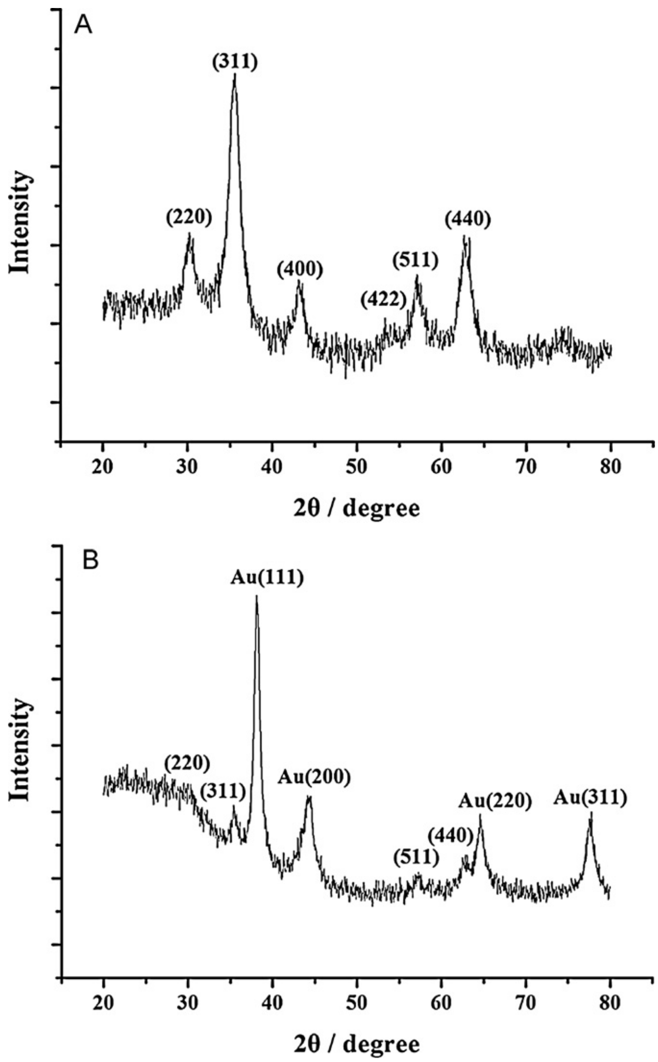

Fig. 3. XRD patterns of (A) Fe_2O_3 and (B) Fe_2O_3@Au MNPs.

of both Au and Fe_2O_3 again verifies the core/shell structure of our Fe_2O_3@Au MNPs.

3.2. Mechanism of electrochemical detection of E. coli

In this paper, Fe_2O_3@Au MNPs were prepared by reducing $HAuCl_4$ on the surfaces of Fe_2O_3 nanoparticles. Based on the Fe_2O_3@Au MNPs an electrochemical DNA biosensor was presented. We employed a "sandwich-type" detection strategy (Scheme 1), which involved capture probe self-assembled at the surface of Fe_2O_3@Au MNPs and biotinylated reporter probe, both of which flank the DNA target sequence. In the presence of target DNA, the capture probe brings the target probe, along with the reporter probe to the proximity of the MNPs. As a result, the biotin tag was localized at the surface of the MNPs, which further brought the avidin-HRP conjugate proximal to the MNPs via the strong biotin–avidin interaction. Of note, one HRP enzyme brought about by one hybridization event could efficiently catalyze thousands of reduction reactions of H_2O_2 with the help of an electroactive co-substrate (TMB) [25], leading to significantly amplified electrochemical signals.

In order to evaluate the selectivity of this method, the sensor was challenged with one-base-mismatched, four-base-mismatched and non-complementary sequence (Fig. 4). The signal produced by the non-complementary oligonucleotide was insignificant from

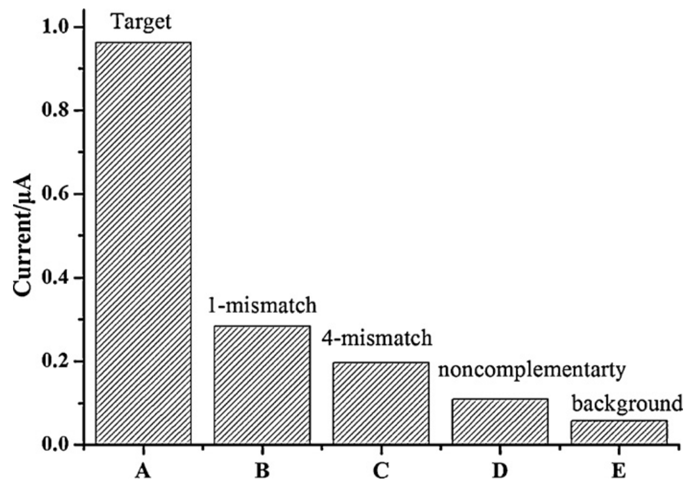

Fig. 4. Comparison for the signal intensity of sensors hybridized with 1 pM complementary target (A), 100 pM one-base-mismatched (B), 100 pM four-base-mismatched (C) and 100 nM non-complementary sequence (D). The hybridization was conducted at 40 °C for 40 min.

the background. The signal for the fully complementary target was at least 3 times larger than that of one-base-mismatched oligonucleotide, suggesting that the enzyme-based DNA sensor is of high sequence specificity toward even a single-base mismatch.

3.3. Optimum conditions for E. coli measurement

DNA hybridization reaction is closely related to the hybridization temperature. Elevated temperature speed the movement of DNA molecules with the hybridization efficiency improved, but on the other hand temperatures higher than the melting temperature (T_m) accelerate the denaturation of dsDNA leading to decreasing current signals. Fig. 5 displays the amperometric signals after hybridization with 10 pM target DNA in the temperature range from 20 to 55 °C. We found hybridization signals were small up to 30 °C and reached maxima at ~40 °C, suggesting that the capture probe was sufficiently hybridized with the target probe. Hence 40 °C was selected for further work.

The effect of the hybridization time was also explored in Fig. 6. As the hybridization time increased from 10 to 50 min,

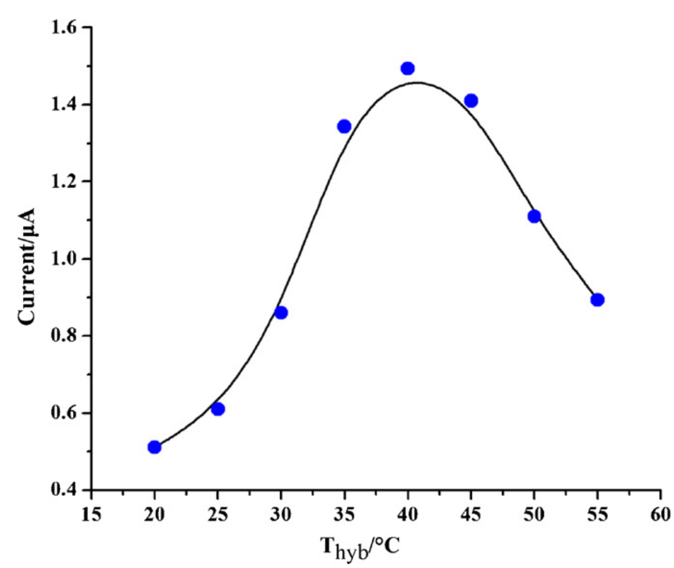

Fig. 5. Amperometric signals obtained with 10 pM target DNA in the temperature range from 20 to 55 °C at 40-min hybridization time.

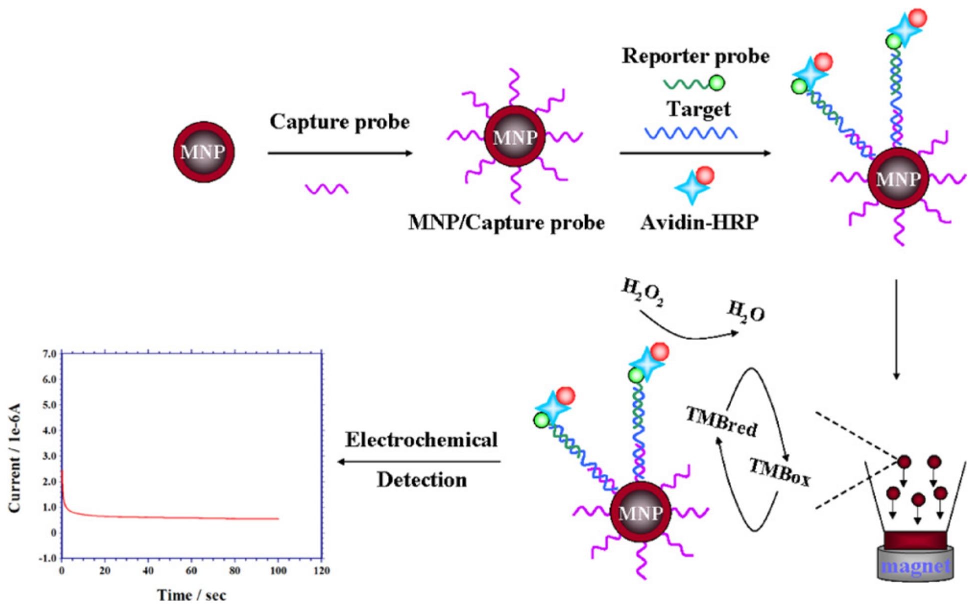

Scheme 1. Schematic drawing for the sandwich-type detection assay of *E. coli* DNA using Fe_2O_3@Au nanoparticles.

the amperometric signal increases gradually (up to 40 min) and then reached a constant lever. As the best compromise between sensitivity and speed, our work employed a 40 min hybridization time.

We challenged the sensor with the synthetic DNA target of a series of concentrations from 0.01 pM to 1.0×10^3 pM. The amperometric signal was found to be a linear logarithmic function related to the target concentration (Fig. 7), spanning a response region of 5 orders of magnitude. The biosensor could detect the DNA target quantitatively in the range of 1.0×10^{-13}–1.0×10^{-9} M with a detection limit of 0.01 pM (>3SD).

3.4. Electrochemical detection of E. coli

The real-life utility of the amperometric DNA assay was illustrated using the detection of *E. coli* DH5α. Fig. 8 displays current–time recordings obtained for samples containing increasing levels of the *E. coli* bacteria from 500 to 5×10^5 cfu/mL. Well-defined amperometric signals are observed for these low levels of *E. coli*. The corresponding calibration plot (Fig. 9) exhibits a linear relationship between the amperometric signal and the log [*E. coli*] ($R^2 = 0.977$). The data of Fig. 8 indicate a detection limit of $500 \pm 5\%$ cfu/mL and the linear range of our electrochemical DNA biosensor was found from 1×10^3 to 5×10^5 cfu/mL. The detection limit obtained in this work was found to be superior to other *E. coli* electrochemical DNA biosensors without a nucleic acid amplification step [16–18].

Further lowering of the detection limit of *E. coli* is achieved by preconcentration and preincubation steps. 1.0 L of *E. coli* cultures were filtrated by filter papers, which were diverted to 50 mL LB medium. The concentrated cultures were incubated for propagation, and withdrawn at 0.5 h intervals for the detection. As can be observed from Fig. 10, 500, 50, and 5 cfu/mL of *E. coli* could be detected after 2.0, 3.0 and 4.0 h incubation, respectively. The current responses increased with the increment of the incubation time,

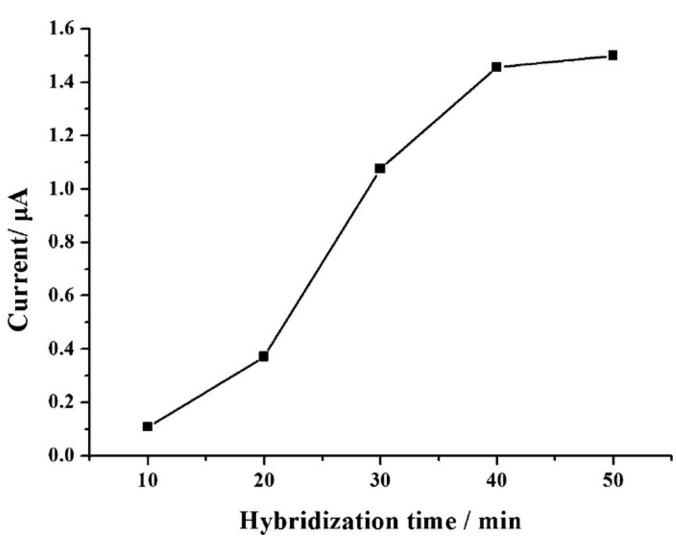

Fig. 6. Amperometric signals changed with the hybridization time while the concentration of target DNA was fixed at 10 pM.

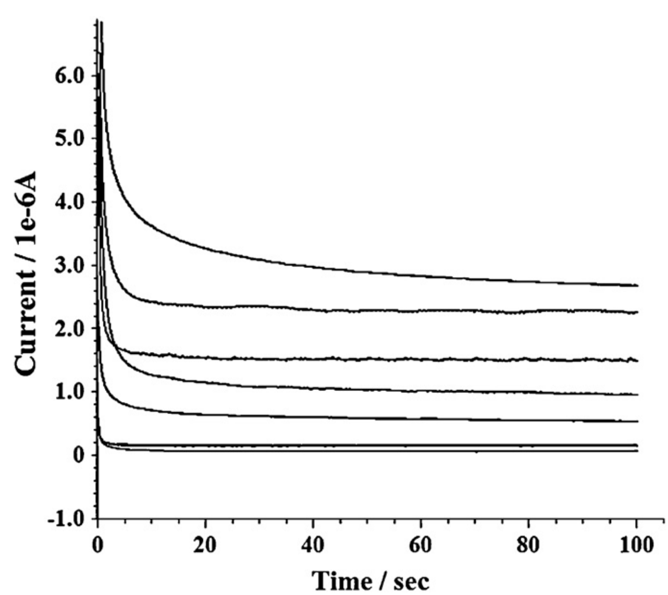

Fig. 7. Amperometric measurements for the detection of synthetic target DNA at a series of concentrations. From bottom to top: background, 0.01 pM, 0.1 pM, 1 pM, 10 pM, 100 pM and 1.0×10^3 pM perfectly matched DNA.

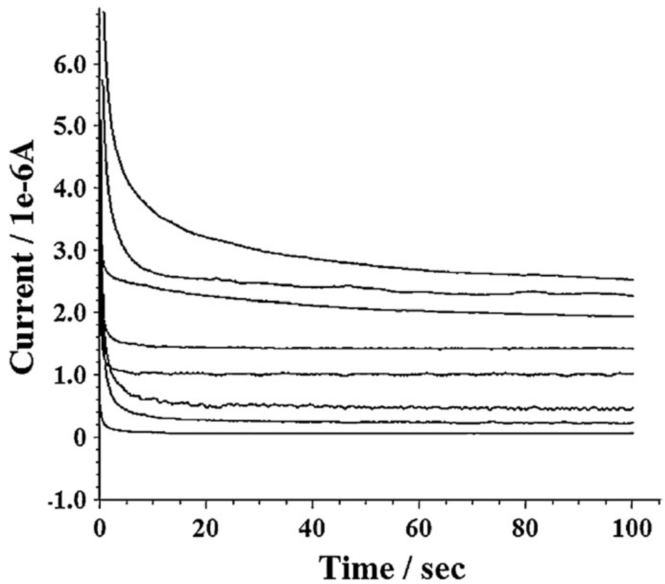

Fig. 8. Amperometric measurements for the detection of *E. coli* at a series of concentrations. From bottom to top: background, 500 cfu/mL, 1×10^3 cfu/mL, 5×10^3 cfu/mL, 1×10^4 cfu/mL, 5×10^4 cfu/mL, 1×10^5 cfu/mL and 5×10^5 cfu/mL of *E. coli*.

and the incubation time required decreased simultaneously when the concentration of bacteria increased.

The repeatability of the biosensor was investigated with a concentration of 5×10^3 cfu/mL of *E. coli*. The relative standard deviation (RSD, $n = 5$) of the current responses was about 4.14%, revealing a good repeatability of the biosensor.

3.5. Detection of E. coli in river water

The method was applied to detect *E. coli* in the river water from our university. A liter of the river water was filtered by 0.45 μm pore sized filter paper and the filter paper was then dipped into flask containing 10 mL LB medium. After 3 h incubation, the bacterial sample was detected by the amperometric method introduced above. The results indicated that the concentration of coliforms in the river water was 100 cfu/mL, which was consistent to the result obtained by plate count method (120 cfu/mL).

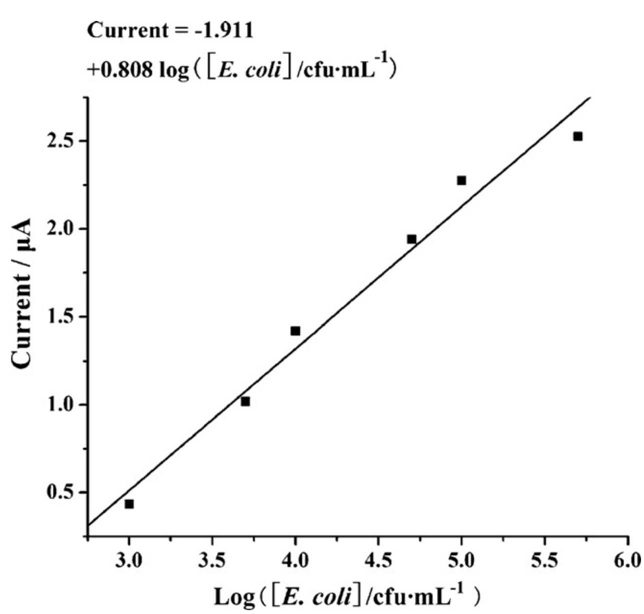

Fig. 9. Logarithmic plot of current vs. *E. coli* concentration.

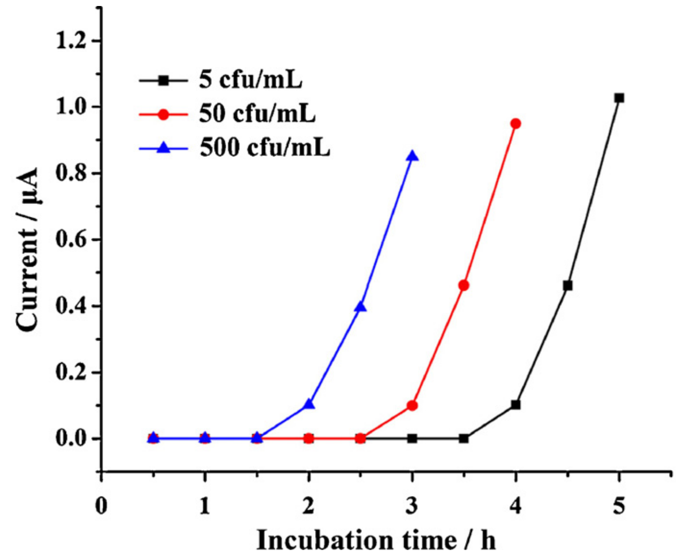

Fig. 10. Current responses of 5, 50 and 500 cfu/mL of *E. coli* after different incubation periods.

4. Conclusion

In this paper, an effective electrochemical DNA biosensor based on Fe_2O_3@Au nanoparticles was demonstrated. These core/shell nanoparticles were shown to have high separation efficiency and can be loaded with large amount of DNA, thus exhibiting improved sensitivity. The biosensor showed good performances in the determination of *E. coli*. Given the low detection limit, cost-effectiveness, enhanced selectivity and good repeatability of this method, we expect it will be a promising tool for the monitoring and surveillance of the bacterial contamination in waters or food industry.

Acknowledgements

We greatly appreciate the financial support of the National Nature Science Foundation of China (20775026), Science and Technology Commission of Shanghai Municipality (No. 1052nm06500) and Shanghai Key Laboratory of Green Chemistry and Chemical Process.

References

[1] E. Bakker, Anal. Chem. 76 (2004) 3285.
[2] J.L. Johnson, B.E. Rose, A.K. Sharar, G.M. Ransom, C.P. Lattuada, A.M. McNamara, J. Food Prot. 58 (1995) 597.
[3] S.H. Kim, M.K. Park, J.Y. Kim, P.D. Chuong, Y.S. Lee, B.S. Yoon, K.K. Hwang, Y.K. Lim, J. Vet. Sci. 6 (2005) 41.
[4] C.X. Lei, S.Q. Hu, N. Gao, G.L. Shen, R.Q. Yu, Bioelectrochemistry 65 (2004) 33.
[5] J.M. Simpson, D.V. Lim, Biosens. Bioelectron. 21 (2005) 881.
[6] C. Bischoff, J. Lüthy, M. Altwegg, F. Baggi, J. Microbiol. Methods 61 (2005) 335.
[7] C. Ruan, L. Yang, Y. Li, Anal. Chem. 74 (2002) 4814.
[8] L. Yang, Y. Li, J. Microbiol. Methods 64 (2006) 9.
[9] S.O. Van Poucke, H.J. Nelis, Appl. Environ. Microbiol. 61 (1995) 4505.
[10] K. Geissler, M. Manafi, I. Amorós, J.L. Alonso, J. Appl. Microbiol. 88 (2000) 280.
[11] J. Wang, G. Rivas, X. Cai, E. Palecek, P. Nielsen, H. Shiraishi, N. Dontha, D. Luo, C. Parrado, M. Chicharro, P.A.M. Farias, F.S. Valera, D.H. Grant, M. Ozsoz, M.N. Flair, Anal. Chim. Acta 347 (1997) 1.
[12] J. Wang, G. Rivas, C. Parrado, X. Xiao, M.N. Flair, Talanta 44 (1997) 2003.
[13] J. Wang, G. Rivas, X. Cai, Electroanalysis 9 (1997) 395.
[14] J. Wang, Biosens. Bioelectron. 21 (2006) 1887.
[15] G.F. Cheng, J. Zhao, Y.H. Tu, P.G. He, Y.Z. Fang, Anal. Chim. Acta 533 (2005) 11.
[16] M.J. LaGier, C.A. Scholin, J.W. Fell, J. Wang, K.D. Goodwin, Mar. Pollut. Bull. 50 (2005) 1251.

[17] J.C. Liao, M. Mastali, V. Gau, M.A. Suchard, A.K. Møller, D.A. Bruckner, J.T. Babbitt, Y. Li, J. Gornbein, E.M. Landaw, E.R.B. McCabe, B.M. Churchill, D.A. Haake, J. Clin. Microbiol. 44 (2006) 561.
[18] J. Wu, K.Y. Chumbimuni-Torres, M. Galik, C. Thammakhet, D.A. Haake, J. Wang, Anal. Chem. 81 (2009) 10007.
[19] O.A. Loaiza, S. Campuzano, M. Pedrero, M.I. Pividori, P. García, J.M. Pingarrón, Anal. Chem. 80 (2008) 8239.
[20] K. Landfester, L.P. Ramírez, J. Phys.: Condens. Matter 15 (2003) S1345.
[21] J. Lin, W. Zhou, A. Kumbhar, J. Wiemann, J. Fang, E.E. Carpenter, C.J. O'Connor, J. Solid State Chem. 159 (2001) 26.
[22] J.L. Lyon, D.A. Fleming, M.B. Stone, P. Schiffer, M.E. Williams, Nano Lett. 4 (2004) 719.
[23] H. Cai, C. Xu, P.G. He, Y.Z. Fang, J. Electroanal. Chem. 510 (2001) 78.
[24] S.B. Darling, S.D. Bader, J. Mater. Chem. 15 (2005) 4189.
[25] G. Liu, Y. Wan, V. Gau, J. Zhang, L.H. Wang, S.P. Song, C.H. Fan, J. Am. Chem. Soc. 130 (2008) 6820.
[26] S. Link, M.A. El-Sayed, J. Phys. Chem. B 103 (1999) 4212.
[27] M.C. Daniel, D. Astruc, Chem. Rev. 104 (2004) 293.
[28] L.L. Pang, J.S. Li, J.H. Jiang, Y. Le, G.L. Shen, R.Q. Yu, Sens. Actuators B 127 (2007) 311.
[29] H. Yu, M. Chen, P.M. Rice, S.X. Wang, R.L. White, S. Sun, Nano Lett. 5 (2005) 379.
[30] M. Mandal, S. Kundu, S.K. Ghosh, S. Panigrahi, T.K. Sau, S.M. Yusuf, T. Pal, J. Colloid Interface Sci. 286 (2005) 187.